Online Fault Location on AC Cables in Underground Transmission Systems using Sheath Currents

C.F. Jensen, O.M.K.K. Nanayakkara, A. D. Rajapakse, U.S. Gudmundsdottir, and C.L. Bak

***Abstract*—This paper studies online travelling wave methods for fault location on a crossbonded cable system using screen currents. During the construction of the electrical connection to the 400 MW off shore wind farm Anholt, it was possible to perform measurements on a 38.4 km crossbonded cable system. At 31.4 km, all cables were accessible which made it possible to apply a fault using an arc free breaker and measure the travelling waves at each end of the cable.**

On a crossbonded cable system, the sheath is short circuited and grounded at both ends. This makes possible the use of low voltage Rogowski coils if the screen currents contain the necessary information for accurate fault location. In this paper, this is examined by analysis of field measurements and through a study of simulations. The wavelet transform and visual inspection methods are used and the accuracy is compared.

Field measurements and simulations are compared for testing the reliability of using simulations for studying fault location methods.

***Index Terms* – Electromagnetic Transients, Cable models, Online Fault Location, Wavelet Transform.**

I. Introduction

Until now, little research has been published on field measurements carried out on crossbonded cable systems using travelling wave of fault location purposes [1]. The reasons for this are that field tests of crossbonded cables are normally destructive and that a cable system is seldom accessible at three locations for testing purposes.

Several issues such as high frequency attenuation in the cables as well as the ability of instrument transformers to represent the measured high voltage signals in the secondary are of great importance for the accuracy of a travelling wave-based fault location method [2] [3]. The classical instrument transformers used today alter the transient signals in the secondary due to inductive, capacitive and non-linear elements in the devices [4] [5] [6]. The result is a distorted signal and the introduction of a a possible time delay. Because the fault created waves in the cable travels with very high velocity and the ability to estimate the exact arrival instance is crucial for accurate fault location, the use of the classical instrument transformers is a potential problem and a better solution is desired.

The sheaths of a crossbonded cable system are short circuited and grounded at each end of the transmission line. This makes the use of low voltage current transducers possible. The Rogowski type of coil is cheap and solid, and comes with a high bandwidth. This type of sensor have been used to capture the surge through surge suppressions capacitors for fault location purposes on DC-systems with success [7]. During the installation of the electrical connection to the 400 MW off shore wind farm Anholt, it was possible to perform measurements on a 38.4 km crossbonded cable system. At 31.4 km, all cables were accessible which made it possible to apply a fault using an arc free breaker and measure the travelling waves at each end of the cable. All three core voltages and currents along with the three sheath current were measured in both ends using a synchronised measuring setup. In this paper, the use of the sheath currents for a travelling wave fault location purpose is examined. The fault surge arrival instance is found through a visual inspection method (VIM) and by the use of the Wavelet Transform method (WTM). Furthermore, to gain knowledge on whether simulations can be trusted for fault location studies done on cables, a highly detailed simulation model is constructed in PSCAD/EMTDC and the results are compared to the measurements.

II. System description and measuring setup

The 245 kV electrical connection to the Anholt offshore wind farm is divided into three cable sections. The first section is a 59.6 km crossbonded land cable from the substation Trige to a newly constructed shunt reactor station close to the beach by the Danish city Grenaa. From the reactor station, a 0.5 km beach cable is used to connect the land cable to the submarine cable. The submarine cable is a three phase cable with a length of 24.5 km. A single line diagram of the system is shown in Figure 1.

It was possible to access the crossbonded land cable at three locations for performing field measurements; at substation Trige (Joint 0), at Joint 27 (31.4 km from Trige) and at Joint 33 (38.4 km from Trige). At Joint 27, all core and sheath conductors were open. This made it possible to apply faults at this location, after the system was energised from Trige with a suitable test voltage, and then measure the travelling

C.F. Jensen is with Energinet.dk Transmission Lines, 7000 Fredericia Denmark (cfj@energinet.dk)

O.M.K.K. Nanayakkara is with the Dept. of Electrical & Computer Engineer University of Manitoba, Winnipeg Canada (umnanayo@cc.umanitoba.ca)

A. D. Rajapakse is with the Dept. of Electrical & Computer Engineer University of Manitoba, Winnipeg Canada (Athula.Rajapakse@ad.umanitoba.ca)

U.S. Gudhmundsdottir is with Energinet.dk, Transmission Lines, 7000 Fredericia Denmark (usg@energinet.dk)

C.L. Bak is with the Dept. of Energy Technology, Aalborg University, 9220 Aalborg (e-mail of corresponding author: clb@et.aau.dk)

Paper submitted to the International Conference on Power Systems Transients (IPST2013) in Vancouver, Canada July 18-20, 2013.)

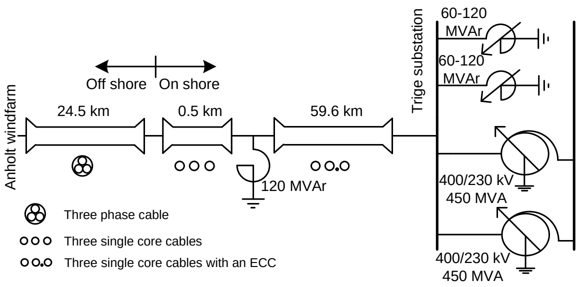

Figure 1. Single line diagram of the electrical connection to the 400 MW Danish off-shore wind farm Anholt.

waves arriving at Joint 0 and Joint 33. In order to apply a fault representing an insulation breakdown, a switch with no pre-strike capability was necessary. A Siemens 3AF 1532-4, 12 kV 1230 A vacuum circuit breaker was selected.
To prevent damaging the cable system during the testing, all measurements were performed at reduced voltage (0.4 kV). The voltage/current relationship of the cable system is linear, so the travelling waves created will be representative for waves created during a real-life fault situation. The system was fed through a 10 kVA 0.4/0.4 kV Dyn transformer setup at Trige. The setup in substation Trige is shown in Figure 2.

Figure 2. Energisation of cable system from a 10 kVA 0.4/0.4 kV Dyn in the substation Trige.

A load resistor was connected to the cable system at Joint 33 to ensure a steady state current flow through the cables prior to the instance of fault. The setup at Joint 33 is shown in Figure 3.

A single line diagram of the part of the system where the measurements are performed is shown in Figure 4.

The cable system consist of three single core aluminum cables with a 170 mm^2 aluminum foil sheath. The physical layout of the single core cable is presented in Figure 5.

The cables are placed in flat formation, and along the system; placed next to phase c, an earth continuity conductor (ECC) is laid. The ECC is a 95 mm^2 insulated copper wire. The layout of the system is presented in Figure 6.

The cable section from Joint 27 to 33 (6.9 km) has two major sections and is crossbonded using a traditional approach, whereas the 31.4 km cable section (Joint 0 to 27) has nine major sections with the three sheaths short circuit at the end of each major section, but grounded only at every second major section.

An internal fault in a cable will always occur when the insulation is most stressed. A case study close to negative peak voltage is therefore presented in this paper.

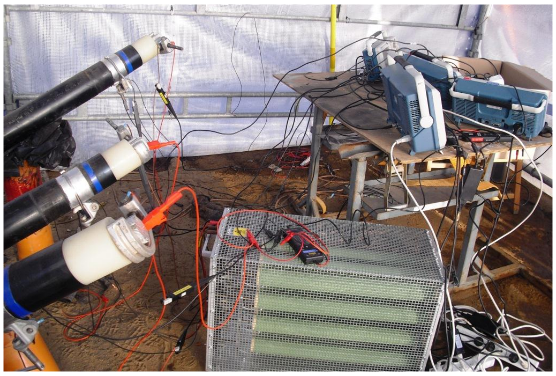

Figure 3. Load resistor connected cable system at Joint 33.

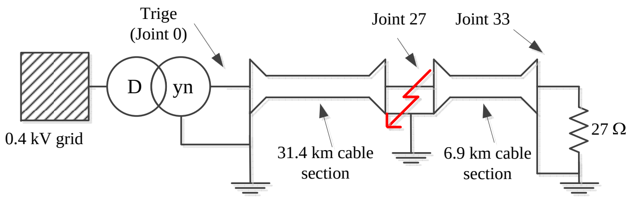

Figure 4. Single line of the 245 kV crossbonded cable system under study.

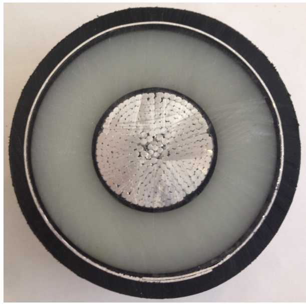

Figure 5. Physical layout of the 2000 mm^2 aluminium single core 245 kV cable.

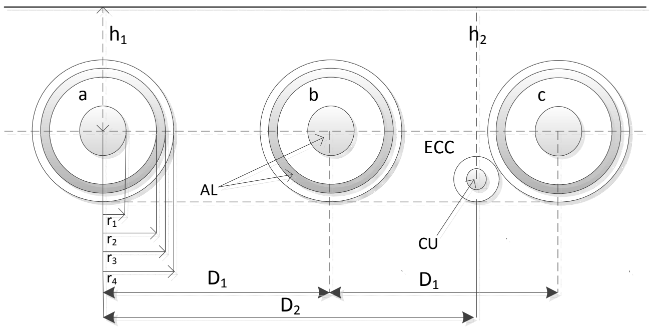

Figure 6. Physical layout of the three phase 2000 mm^2 aluminium single core 245 kV crossbonded cable system. $r_1 = 28.4$ mm, $r_2 = 35.9$ mm, $r_3 = 54.4$ mm, $r_4 = 58.6$ mm, $\rho_c = 3.547e^{-8}$ Ωm, $\rho_s = 2.676$ Ωm, $\rho_{ECC} = 1.724e^{-8}$ Ωm, , $\rho_E = 100$ Ωm $\epsilon_{i1} = 2.89$, $\epsilon_{i2} = 2.3$, $\epsilon_{ECC} = 2.3$, $D_1 = 0.4$ m, $D_2 = 0.75$ m, $h_1 = 1.3$m, $h_2 = 1.3511$m.

A. Modal decomposition

For most high frequency fault location methods, the wave propagation velocity is a required parameter. The conductors in a three phase cable system form many loops of different sizes and therefore, a single velocity does not exist. Nor can a unique reflection or refraction coefficient be calculated for each conductor. Therefore, the modal decomposition theory was developed [8]. This method utilises frequency dependent eigenvalues and transformation matrices, allowing the n conductor transmission system to be represented as n independent conductors [9].

At high frequencies, a three phase cable system with an ECC will, after the modal decomposition, be represented by three coaxial, three intersheath ECC and one ground mode. In [10], the coaxial wave velocity was identified as the modal velocity best suited for fault location purposes as it is the fastest of all frequencies, and the velocity of the mode becomes frequency independent at fault frequencies. The coaxial type of wave can be used for measurements carried out on the sheath circuit as well, as the coaxial wave is defined as a wave travelling between the core and the sheath closest to it [10]. A coaxial current wave will therefore travel on the sheath from the fault location and towards the cable ends where it can be picked up and used to determine the fault location.

The modal velocity used in this article is calculated using the modal decomposition theory and measured on the actual cable system using an impulse test method described in [10].

B. Measuring system

High bandwidth measuring equipment was used for capturing the arrival instances of the travelling waves on the cable system after the breaker had been closed. Two different current probes are used at Joint 0 and 33. At Joint 0, a Tektronix TCP0150 probe is used where at Joint 33, a TCP0030 probe is used. The current range and bandwidth are shown in Table I.

Table I
DATA FOR CURRENT PROBES USED TO OBTAIN SHEATH CURRENTS AT JOINT 0 AND 33.

	TCP0030	TCP0150
RMS current (peak)	30 A (50 A)	150 A (500 A)
Bandwidth	DC to 120 MHz	DC to $>$ 20 MHz

In an practical implementation, current sensors with adequate bandwidth can be realised using the Rogowski type of sensor.

The signals were recorded with Tektronix DPO2014 oscilloscopes set at a sampling frequency of 10 MHz. The vertical resolution of the oscilloscopes was 8 bits or 256 points. To synchronise the two measuring locations, synchronisation units and are based on the Rubidium frequency standard were used [11].

III. SIMULATION MODEL

A model of the system is built in the transient simulation program PSCAD/EMTDC. The cables are modelled using the frequency dependent (phase) model and a detailed implementation of the crossbonding is carried out as described in [12]. The parameters given to the cable model are taken from the data sheet and based on a geometric description of the cables. The core and sheath resistivities and the main insulation permittivity are corrected using the methods presented in [13]. An ideal resistor is used to represent the load, and the standard two winding transformer model available in the PSCAD library represents the 0.4 kV transformer at Trige. The grounding resistances at the crossbonding locations are modelled as 10 Ω resistances where the grounding resistance at substation Trige is set to 0.1 Ω. All simulations are run until steady state is reached before a fault is applied.

IV. SYNCHRONISED TWO TERMINAL FAULT LOCATION METHOD

The classical synchronised two terminal fault location algorithm is shown in 1.

$$x = \frac{l_c - v_c \cdot \tau_d}{2} \qquad [\mathrm{m}] \tag{1}$$

where v_c is the propagation velocity for the coaxial mode, l_c is the length of the cable line, and τ_d is the time difference between the arrival instance of the first coaxial wave at Joint 33 and 0 $(\tau_{C1,33} - \tau_{C1,0})$.

The expected theoretical arrival instance of the first coaxial at Joint 0 and 33 for a fault occurring at Joint 27 at $t = 0$, based on the modal velocity calculated based on cable parameters and the velocity determined using the impulse test are presented in Table II.

Table II
EXPECTED THEORETICAL AND MEASURED ARRIVAL INSTANCE OF FIRST AND SECOND COAXIAL WAVE FROM FAULT LOCATION.

Reflection	Theoretical instance [μs]	Measured instance [μs]
$\tau_{C1,0}$	177.74	181.24
$\tau_{C1,33}$	39.07	39.84

The instance the fault is applied is unknown relative to the wave recorded at Joint 0 and 33 - only the time difference $(\tau_{C1,33} - \tau_{C1,0})$ can be determined for the measured signals. The time difference which will lead to a correct fault location is -141.4 μs using the measured velocity as input and -138.67 μs for the velocity calculated based on cable parameters.

V. FAULT LOCATION ON CROSSBONDED CABLE SYSTEMS

The visual inspection method requires that the sheath current signals are recorded at both ends using an appropriate data acquisition system with the capability to self trigger and record the signals in sufficient time. The signals are sent to an operator who determines the arrival instance manually.

The wavelet method can be used directly on the time domain signals as well, but without the interference of an operator. The advantage of using the WTM is that a fault location is calculated directly and no skilled operator is necessary. The WTM can, however, be sensitive to noise, and a wrong trigger signal will result in a wrong fault location. This can be expensive if no further estimation of the fault location is carried out. The use of an operator ensures that no faulted trigger signals are used for calculating the fault location. Furthermore, an operator will most likely be better at determining when the waves arrive based on experience with the VIM. In the following sections, both methods are examined.

A. Visual inspection method (VIM)

In Figure 7, the simulated and measured sheath current signals at Joint 0 and 33 are shown after a single core-to-sheath-to-ground fault is applied at Joint 27.

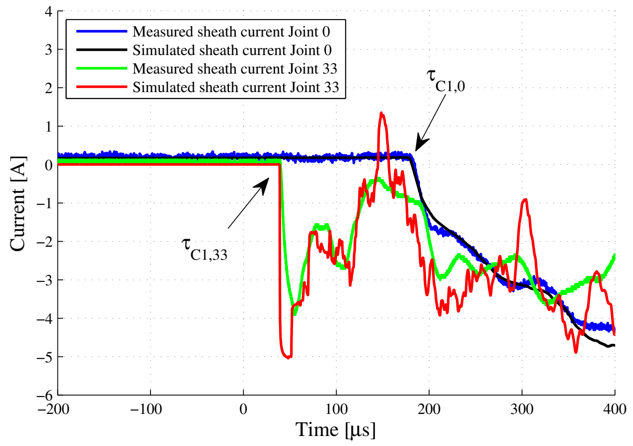

Figure 7. Low time resolution plot of sheath currents measured at Joint 0 and 33 after a fault has been applied at $t = 0$.

The effect of different current probes in Joint 0 and 33 are clearly seen in the figure. Higher current range along with the relative low vertical resolution of the oscilloscopes make it harder to precisely identify wave front arrival time. At Joint 33 (6.9 km from the fault location), the measured sheath current shows a much higher degree of damping compared to simulations. The surge impedance of the load and transformer will together with the cables coaxial surge impedance determine the sheath current profile until the first intersheath mode waves arrives at both locations. The load resistor is modelled in PSCAD/EMTDC as a real resistor, but in real-life it will show inductive behaviour due to its coil-like construction. The current cannot instantaneously build up through the windings, thus making the current sloop less steep compared to simulations. The inductance will be frequency dependent due to current displacement and as such an advanced model is not available in PSCAD/EMTDC and because the implementation is not important for the results of this work, it is not studied in detail in this paper.
Other parameters affecting the damping in the cable system are discussed in detail in [2].
At Joint 0, the degree of damping is high, but equal in both the simulated and measured signals. The standard transformer model provided in PSCAD performs well at lower frequencies and the measured and simulated results are very similar. In Figure 8, a high time resolution plot of the sheath current signals recorded at Joint 33 are seen.

The arrival instance based on the times displayed in Table II are marked in the figure. Due to damping, it is difficult to determine the exact arrival instance in the measured signal. In order to address this problem, an interval is defined by the operator in which it is most likely the fault wave has arrived. The interval is marked in the figure and has a length of 0.35 μs for this case. In Figure 9 the high time resolution plot of the sheath current signals recorded at Joint 0 are seen.

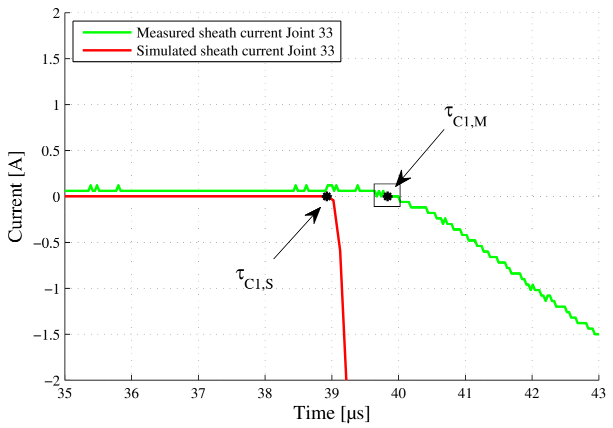

Figure 8. High time resolution plot of sheath currents measured at Joint 33 after a fault has been applied at $t = 0$.

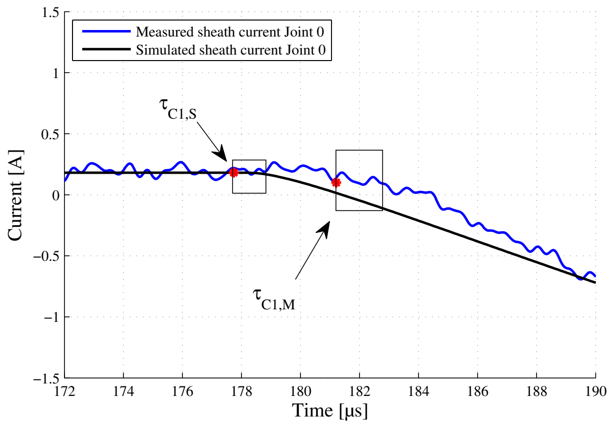

Figure 9. High time resolution plot of sheath currents measured at Joint 0 after a fault has been applied at $t = 0$.

In Figure 9, it can be seen how accurate arrival time cannot be identified by a single number. It is therefore important to use intervals with the arrival time. For the simulated signals, this is due to attenuation alone, where for the measured signals, it is both due to attenuation and digital quantification problems. Using two vector inputs in (1), results in a matrix with possible fault locations. The maximum and minimum values in the matrix are identified and will define an interval in which the fault most likely will be located. The same is done for the simulated intervals. In the case of simulated signals using the VIM, the real fault location is not found in the interval. The fault location is, however, only 6 m outside the interval. Ideally, the fault location should be in the middle of the interval. The reason it is not is because of the difficulties in determining the arrival instance at Joint 0 where the high frequency components are strongly damped. Using the VIM on the measured signals, the fault location is correctly determined to lie within the interval, but the interval is screwed towards the same end as in the case of the measurements. This indicates that an experienced operator would be able to compensate for this by judging the degree of damping.

B. Wavelet transform method (VTM)

Wavelet transform works well for analysing transients in signals because of its simultaneous time and frequency localisation capabilities, and it has been widely used in fault location applications [14]-[18]. In the case of the wavelet transform, the analysing functions are called mother wavelets and are defined as (2).

$$\varphi_{p,\tau} = \frac{1}{\sqrt{p}}\varphi^*\left(\frac{t-\tau}{p}\right) \tag{2}$$

A given mother wavelet φ has a location or time shift τ and a scale or duration p. In the wavelet transform, these shift and scale values are adjusted. In this study, the 'haar' mother-wavelet was selected based on its performance, and it is considered the simplest mother wavelet type available. Therefore, it may require less computation power and resources when implementing in hardware. Continuous wavelet transform (CWT) was used in this study, and the relative merits of using the CWT are discussed in detail in [16]. The wavefront arrival can be recognised by analysing the CWT coefficients of measured terminal sheath current signals. Magnitudes of the CWT coefficients of the input signal were calculated at scales 128 (this corresponds to 0-78.1kHz frequency band) at each terminal. Selection of proper scale is a tradeoff between the time accuracy and noise immunity as discussed in [16]. Surge arrival point is clearly visible by the sharp change in the CWT coefficients of both ends of the input signals. A threshold to identify the wave front arrival point is set 20% above the maximum value of the corresponding signal (CWT coefficient) under normal conditions. The safety margins are required to allow for the noise. In Figure 10, the time domain and Wavelet Transform of the sheath currents recorded at Anholt are presented.

The Wavelet Transform with the given thresholds determines the arrival instances $\tau_{C1,0} = 179.61\ \mu$s and $\tau_{C1,33} = 34.55\ \mu$s. This results in a fault location estimated at 31.731 km from Joint 0 - an error of -317 m. Figure 10 shows that the threshold for the signal at Joint 0 has to be selected much higher compared to Joint 33 because of the noise. This lowers the accuracy and shows the importance of selecting well scaled measuring equipment.

C. Field measurement results

The fault location is determined quite accurately using the automated method based on the Wavelet Transform. However, to limit potentially wrong fault location determinations caused by a wrong automised analysis, a hybrid method is recommended by the authors. The Wavelet Transform is useful in providing the trigger signal for the digital fault recorders and to provide a first estimate of the fault location. It is, however, beneficial for skilled personnel. to analyse the time domain signals after they are recorded to determine whether faulted triggers have occurred and to adjust the time instances selected by the WTM.

The estimated fault location, the length of the estimated interval and the absolute error are presented in Table III using both the VIM and the WTM.

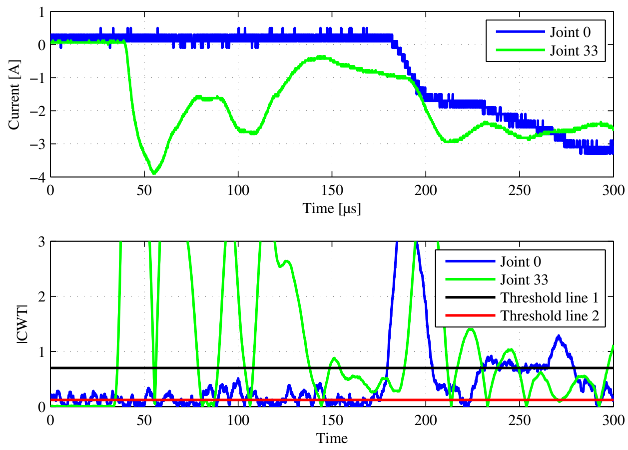

Figure 10. (a) Time domain and (b) Continuous Wavelet Transform at scale 128 using the Haar Wavelet of sheath currents measured at Joint 0 and 33 after a fault has been applied at $t = 0$.

Table III
THE ESTIMATED FAULT LOCATION INTERVAL, THE LENGTH OF THE ESTIMATED INTERVAL AND THE ABSOLUTE ERROR USING THE VIM AND THE WTM.

	Fault location interval [km]	Interval length [m]	Estimation Error [m]
Simulated (VIM)	[31.426, 31.483]	57	[12, 69]
Simulated (WTM)	31.522	-	-109
Measured (VIM)	[31.381, 31.557]	174	[-32, 142]
Measured (WTM)	31.731	-	-317

The results of both the simulations and measurements show that the sheath current can be used for fault location purposes if the currents are measured using suitable transducers and fault recorders. However, care should be taken for longer cables as high frequency attenuation can be a problem.

VI. FAULT LOCATION ON 60 KM CABLE

In order to examine the accuracy of the VIM and WTM on longer cable sections with several different fault locations, a full model of the 60 km land cable part seen in Figure 1 is implemented in PSCAD/EMTDC. Joint faults (core/sheath/ground) are applied at 1.163 km, 17.235 km, 31.415 km, 48.891 km and 55.938 km from Terminal A. The sheath currents are synchronised and sampled at 10 MHz at each cable end. Results using the VIM based on selection of a specific arrival instance are compared to the automated results obtained using the WTM. The estimated fault location (EFL) and the absolute and relative error are presented in Table IV.

Using the VIM, the fault is located quite accurately. The worst case is Case 1 and 5 where one of the fault waves has to travel the longest distance and therefore will be subjected to most damping. This shows that there is a maximum cable length on which a travelling wave fault location method using sheath current will give accurate results.
The WTM generally gives less accurate results, but the interference of an operator is not necessary.

Table IV
THE ESTIMATED FAULT LOCATION INTERVAL, THE ABSOLUTE ERROR AND THE RELATIVE ERROR FOR CASE STUDIES CARRIED OUT ON THE 60 KM ANHOLT CABLE USING THE VIM AND WTM.

	FL	EFL [km]	Error [m]
VIM	1.163	0.975	188
	17.235	17.129	106
	31.415	31.427	-12
	48.891	48.942	-51
	55.938	56.118	-181
WTM	1.163	0.966	197
	17.235	17.244	-9
	31.415	31.577	-162
	48.891	49.225	-334
	55.938	56.338	-401

VII. CONCLUSION

In this paper, the use of screen current signals for online fault location on a crossbonded cable system was examined. Filed measurements of a fault occurring on a 38 km crossbonded cable connecting the 400 MW offshore wind farm Anholt to the main Danish transmission grid was analysed for fault location purposes. Two method for fault location are proposed. First, a visual inspection methods where an operator analyses a time domain representation of the sheath current signals, and based on a subjective judgment, determines the arrival instances of the fault created travelling waves. To deal with noise and damping issues, an interval containing the most likely arrival instances of the fault wave is defined. The result is an interval containing the most likely fault location. The method is robust and gives very accurate results, but it requires that the signals are recorded at a high sampling frequency in an appropriate time interval.
An automated method based on Wavelet Transform is proposed as well. The method gives good results under normal operation; however, it is sensitive to noise in the signal. This can lead to faulted triggers and an incorrect fault location can be proposed by the algorithm. In order to address this problem, a hybrid method is proposed.
To verify the proposed methods, a 60 km crossbonded cable is implemented in PSCAD/EMTDC and fault location studies are carried out. Both methods give acceptable results with maximum deviations of 0.32 % and 0.67 % of the total cable length using the visual inspection and Wavelet based methods respectively.

REFERENCES

[1] D. Spoor and J. G. Zhu, "Improved single-ended traveling-wave fault-location algorithm based on experience with conventional substation transducers," *Power Delivery, IEEE Transactions on*, vol. 21, no. 3, pp. 1714 –1720, july 2006.

[2] U. S. Gudmundsdottir, *Modeling of long High Voltage AC cables in Transmission Systems*, 2nd ed. Energinet.dk, 2010, iSBN 978-87-90707-73-6.

[3] M. Gilany, D. khalil Ibrahim, and E. S. T. Eldin, "Traveling-wave-based fault-location scheme for multiend-aged underground cable system," *Power Delivery, IEEE Transactions on*, vol. 22, no. 1, pp. 82 –89, jan. 2007.

[4] "Transient response of coupling capacitor voltage transformers ieee committee report," *Power Apparatus and Systems, IEEE Transactions on*, vol. PAS-100, no. 12, pp. 4811 –4814, dec. 1981.

[5] "Transient response of current transformers," *Power Apparatus and Systems, IEEE Transactions on*, vol. 96, no. 6, pp. 1809 – 1814, nov. 1977.

[6] M. Kezunovic, L. Portillo, G. Karady, and S. Kucuksari, "Impact of optical instrument transformer characteristics on the performance of protective relays and power quality meters," in *Transmission Distribution Conference and Exposition: Latin America, 2006. TDC '06. IEEE/PES*, aug. 2006, pp. 1 –7.

[7] P. Chen, B. Xu, and J. Li, "A traveling wave based fault locating system for hvdc transmission lines," in *Power System Technology, 2006. PowerCon 2006. International Conference on*, oct. 2006, pp. 1 –4.

[8] H. W. Dommel, *EMTP Theory Book*, 2nd ed. Microtran Power System Analysis Corporation, 1996.

[9] H. Dommel, "Digital computer solution of electromagnetic transients in single-and multiphase networks," *Power Apparatus and Systems, IEEE Transactions on*, vol. PAS-88, no. 4, pp. 388 –399, april 1969.

[10] C. Jensen, U. Gudmundsdottir, C. Bak, and A. Abur, "Field test and theoretical analysis of electromagnetic pulse propagation velocity on crossbonded cable systems," *Power Delivery, Unpublished, revised manuscript submitted in August 2012, IEEE Transactions on*.

[11] S. R. Systems, *PRS10 Rubidium frequency standard with low phase noise*, 2012.

[12] C. Jensen, F. Faria da Silva, C. Bak, and W. Wiechowski, "Switching studies for the horns rev 2 wind farm main cable," *International Conference on Power Systems Transients (IPST)*, 2011.

[13] B. Gustavsen, J. Martinez, and D. Durbak, "Parameter determination for modeling system transients-part ii: Insulated cables," *Power Delivery, IEEE Transactions on*, vol. 20, no. 3, pp. 2045 – 2050, july 2005.

[14] F. Magnago and A. Abur, "Fault location using wavelets," *Power Delivery, IEEE Transactions on*, vol. 13, no. 4, pp. 1475 –1480, oct 1998.

[15] R. Keswani, "Identification of fault in hvdc converters using wavelet based multi-resolution analysis," in *Emerging Trends in Engineering and Technology, 2008. ICETET '08. First International Conference on*, july 2008, pp. 954 –959.

[16] O. Nanayakkara, A. Rajapakse, and R. Wachal, "Location of dc line faults in conventional hvdc systems with segments of cables and overhead lines using terminal measurements," *Power Delivery, IEEE Transactions on*, vol. 27, no. 1, pp. 279 –288, jan. 2012.

[17] A. Borghetti, S. Corsi, C. Nucci, M. Paolone, L. Peretto, and R. Tinarelli, "On the use of continuous-wavelet transform for fault location in distribution power systems," *International Journal of Electrical Power and Energy Systems*, vol. 28, pp. 608–617., 2006.

[18] O. Nanayakkara, A. Rajapakse, and R. Wachal, "Fault location in extra long hvdc transmission lines using continuous wavelet transform," *International Conference on Power Systems Transients (IPST2011)*, 2011.